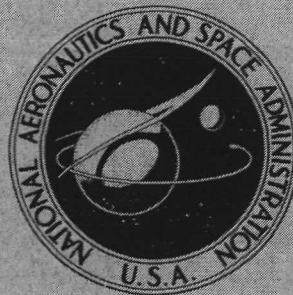


NASA TECHNICAL
MEMORANDUM



N73-30864
NASA TM X-2909

NASA TM X-2909

CASE FILE
COPY

STATUS OF TWO STUDIES
ON ACTIVE CONTROL OF
AEROELASTIC RESPONSE

by Irving Abel and Maynard C. Sandford

Langley Research Center

Hampton, Va. 23665

1. Report No. NASA TM X-2909	2. Government Accession No.	3. Recipient's Catalog No.	
4. Title and Subtitle STATUS OF TWO STUDIES ON ACTIVE CONTROL OF AEROELASTIC RESPONSE		5. Report Date September 1973	6. Performing Organization Code
		8. Performing Organization Report No. L-9251	10. Work Unit No. 743-36-04-01
7. Author(s) Irving Abel and Maynard C. Sanford		11. Contract or Grant No.	13. Type of Report and Period Covered Technical Memorandum
9. Performing Organization Name and Address NASA Langley Research Center Hampton, Va. 23665		14. Sponsoring Agency Code	
		12. Sponsoring Agency Name and Address National Aeronautics and Space Administration Washington, D.C. 20546	
15. Supplementary Notes			
16. Abstract <p>The application of active control technology to the suppression of flutter has been successfully demonstrated during two recent studies in the Langley transonic dynamics tunnel. The first study involved the implementation of an aerodynamic-energy criterion, using both leading- and trailing-edge controls, to suppress flutter of a simplified delta-wing model. Use of this technique has resulted in an increase in the flutter dynamic pressure of approximately 12 percent for this model at a Mach number of 0.9. Analytical methods used to predict the open- and closed-loop behavior of the model are also discussed. The second study, which is a joint effort with the Air Force Flight Dynamics Laboratory, was conducted to establish the effect of active flutter suppression on a model of the Boeing B-52 Control Configured Vehicle (CCV). Some preliminary results of this study indicate significant improvements in the damping associated with the critical flutter mode.</p>			
17. Key Words (Suggested by Author(s)) Active control Aeroelastic response		18. Distribution Statement Unclassified - Unlimited	
19. Security Classif. (of this report) Unclassified	20. Security Classif. (of this page) Unclassified	21. No. of Pages 29	22. Price* Domestic, \$3.00 Foreign, \$5.50

STATUS OF TWO STUDIES ON ACTIVE CONTROL OF AEROELASTIC RESPONSE

By Irving Abel and Maynard C. Sandford
Langley Research Center

SUMMARY

The application of active control technology to the suppression of flutter has been successfully demonstrated during two recent studies in the Langley transonic dynamics tunnel. The first study involved the implementation of an aerodynamic-energy criterion, using both leading- and trailing-edge controls, to suppress flutter of a simplified delta-wing model. Use of this technique has resulted in an increase in the flutter dynamic pressure of approximately 12 percent for this model at a Mach number of 0.9. Analytical methods used to predict the open- and closed-loop behavior of the model are also discussed. The second study, which is a joint effort with the Air Force Flight Dynamics Laboratory, was conducted to establish the effect of active flutter suppression on a model of the Boeing B-52 Control Configured Vehicle (CCV). Some preliminary results of this study indicate significant improvements in the damping associated with the critical flutter mode.

INTRODUCTION

Considerable interest has emerged over the last few years toward applying active control technology to suppress aeroelastic response of present and future aircraft configurations. Potential gains in aerodynamic efficiency and weight savings can be realized through ride-quality control, reduction of gust and maneuver loads with a consequent reduction in fatigue damage, reduction of static-stability requirements, and suppression of flutter. The use of active controls to suppress aeroelastic response is not new. It has already been used, to a limited degree, on such airplanes as the XB-70 and B-52 to improve ride quality by reducing structural response to turbulence (refs. 1 and 2).

The use of active controls to suppress flutter seems further from realization than other active control concepts, partly because of the lack of a thorough experimental evaluation. A review of the recent literature (e.g., refs. 3, 4, and 5) indicates that most of the work in this area is analytical. In an effort to fill the need for experimental results, wind-tunnel model programs are underway in the Langley transonic dynamics tunnel to demonstrate the effectiveness of using active controls for flutter suppression.

The purpose of this paper is to describe some recent activities at Langley Research Center toward evaluating the use of active controls for flutter suppression. (Some early progress on these programs was reported in ref. 6.) The application of active controls to the suppression of flutter at transonic speeds on a simplified delta-wing model is described. Included is a brief summary of the analytical aspects of the problem, a description of the model, measured and calculated flutter points with and without active controls, and some experimental techniques used to establish the behavior of the model at subcritical test conditions.

In addition to the delta-wing program, a program is being conducted to evaluate the use of active controls for flutter suppression, maneuver-load control, ride-quality control, and reduction of static-stability requirements on a model of the Boeing B-52 CCV airplane. This program is a cooperative effort by Langley Research Center; the Air Force Flight Dynamics Laboratory; and The Boeing Company, Wichita Division, under NASA and Air Force contracts. These studies are being conducted in conjunction with a flight research program (ref. 7) in an effort to correlate model and flight data. This paper includes a brief summary of preliminary wind-tunnel flutter-suppression studies accomplished to date.

SYMBOLS

b	reference semichord
c	reference chord, $2b$
f_A, f_B	frequencies at half-power points of forced response
g	structural damping coefficient
$h(x,y,t)$	vertical displacement
h_1, h_2	vertical displacement of delta-wing model at 30 and 70 percent of the reference chord, respectively (fig. 5)
M_i	generalized mass of i th vibration mode
$m(x,y)$	mass distribution
$\Delta p(x,y,t)$	pressure distribution

q_i	generalized displacement of ith vibration mode
S	reference area
s	Laplace operator
t	time
U	aerodynamic-energy matrix defined in equation (2)
\bar{U}	complex conjugate of the matrix U
V	free-stream velocity
x,y	streamwise and spanwise coordinates, respectively
$Z_i(x,y)$	normalized deflection in ith vibration mode
α	angle of attack at section A-A (fig. 5)
β	leading-edge-control deflection
δ	trailing-edge-control deflection
δ_a	B-52 outboard-aileron deflection
$\delta_{a,c}$	deflection command signal to B-52 outboard aileron
δ_f	B-52 flaperon deflection
$\delta_{t,c}$	deflection command signal to delta-wing trailing-edge control
ω	circular frequency

Matrix notation:

$\{ \}$	column matrix
$[\]$	row matrix

[] square matrix

[]^T transpose of matrix

Dots above symbols indicate derivatives with respect to time.

FLUTTER SUPPRESSION BASED ON AERODYNAMIC ENERGY CONSIDERATIONS

Flutter is a self-excited oscillation in which energy is absorbed by the lifting surface from the airstream. The state of stability of the system is defined by the sign of the work per cycle when the lifting surface undergoes an arbitrary oscillatory motion. The use of energy techniques to investigate the stability of an aeroelastic system is not new (ref. 8); however, a recent contribution to the area of flutter suppression is the development of an aerodynamic energy criterion by Nissim (ref. 3). This criterion states that a necessary and sufficient condition for the prevention of flutter is that for all allowable oscillatory motions of an elastic system in an airstream, positive work must be done by the system on the surrounding airstream. A brief summary of the salient points brought out in reference 3 is given in the following section.

Energy Concept

Consider the equations of motion for a system with n degrees of freedom:

$$\{\ddot{F}\} = -\omega^2 \left[[M] + \pi \rho b^4 S \left[[A_R] + i [A_I] \right] \right] \{q\} + [K] \{q\} \quad (1)$$

where, at flutter, the generalized force $\{F\} = 0$ and ω is the circular frequency of oscillation; $[M]$ is the mass matrix (called B in ref. 3); $[A_R]$ and $[A_I]$ are the real and imaginary unsteady aerodynamic-force matrices, respectively; $[K]$ is the structural stiffness matrix (called E in ref. 3); ρ is the fluid density; S and b are a reference area and length, respectively; and $\{q\}$ is the generalized displacement vector.

Nissim shows that the work per cycle W (called P in ref. 3) done by the system on the airstream can be written as

$$W = \frac{1}{2} \pi^2 \rho b^4 S \omega^2 \left[q_R - i q_I \right] [U] \left\{ q_R + i q_I \right\} \quad (2)$$

where

$$\{q\} = \{q_R + iq_I\} e^{i\omega t}$$

and

$$[U] = \left[-\left[[A_I] + [A_I]^T \right] + i \left[[A_R] - i [A_R]^T \right] \right]$$

A positive value for W indicates a transfer of energy from the system to the airstream, and hence stability. The matrix U is Hermitian (i.e., $\bar{U}^T = U$) and therefore possesses real eigenvalues. By use of these eigenvalues it is shown in reference 3 that the energy input per cycle into the airstream can be reduced to a principal quadratic form as

$$W = \frac{1}{2} \pi^2 \rho b^4 \omega^2 S \left[\lambda_1 (\xi_{R_1}^2 + \xi_{I_1}^2) + \lambda_2 (\xi_{R_2}^2 + \xi_{I_2}^2) + \dots + \lambda_n (\xi_{R_n}^2 + \xi_{I_n}^2) \right] \quad (3)$$

where $\lambda_1, \lambda_2, \dots, \lambda_n$ are the eigenvalues of the matrix U and ξ denotes generalized coordinates associated with the aerodynamic energy. It can be seen from equation (3) that the work W will always be positive if all the eigenvalues λ are positive. Therefore, a sufficient condition for flutter stability is that all the λ terms are positive. A notable characteristic of the energy method is that the criterion for flutter stability is determined by the characteristics of the aerodynamic-force matrices alone. Therefore, if a particular system has undesirable flutter characteristics (i.e., too low a flutter speed), the flutter characteristics can be improved if a mechanism can be found which changes the U matrix in an appropriate manner. One such mechanism is the addition of control surfaces to the basic system. The motions of these surfaces generate aerodynamic forces which modify the aerodynamic terms in the U matrix for the basic system. For flutter suppression the control-surface deflections are related by a "control law" to the plunging and pitching motion of the main surface. Nissim points out in reference 3 that a suitable configuration is one employing both leading- and trailing-edge controls since the two working together provide independent control of lift and pitching moment.

Delta-Wing Flutter Suppression Model

To evaluate the practical aspects of the aerodynamic-energy concept, The Boeing Company, Wichita Division, under contract to NASA, performed an analytical study of the application of this concept to an early supersonic transport (SST) configuration. Some results of this study, as described in reference 9, indicate increases in the flutter speed, from 11 to 29 percent for several spanwise locations of leading- and trailing-edge controls.

Because of these positive results, an experimental program aimed at providing evaluation and validation of the energy concept was initiated by using a wall-mounted 1/17-size simplified semispan model of a recent SST configuration. The Boeing Company, under contract to the Langley Research Center, is providing general support for this program in the area of controls implementation and analysis. A photograph of the model installed in the Langley transonic dynamics tunnel is shown in figure 1, and a sketch of the model is presented in figure 2.

The wing has a clipped-delta planform without twist or camber, a symmetric circular-arc airfoil section with a maximum thickness-to-chord ratio of 0.03, and hydraulically actuated leading- and trailing-edge controls. The trailing-edge control was approximately 20 percent of the local chord, while the leading-edge control varied from about 15 percent of the chord inboard to 20 percent of the local chord outboard. Both controls were located between 73 and 84 percent of the wing span. These locations are approximately those referred to in reference 9 that resulted in the largest increase in flutter speed. Simulated engine nacelles are mounted on the underside of the wing. The model construction consists of an internal aluminum alloy plate that was tapered in thickness in the spanwise direction and had cutouts to simulate spars and ribs. The plate was covered with balsa wood to provide the proper aerodynamic contour.

Because of the large hinge moments required and the necessity of keeping the control-surface actuation system within the physical constraints imposed by the model, that is, small and light, it was necessary to design and fabricate an electrohydraulic actuation system. Within these constraints an actuator was designed that weighs only 56.7 grams yet can produce approximately 4.52 N-m of torque throughout the operating range of interest (approximately from 0 to 25 Hz). Because of the limited thickness of the wing, it was also necessary to design and fabricate special control-surface position indicators. This was accomplished by mounting silicon solar cells to the actuator control shaft and illuminating them with a stationary light source. As the control shaft rotates, a voltage proportional to the angular position of the surface is produced. A photograph of the model showing the actuator and position indicator is presented in figure 3. A complete description of the design and fabrication of the control actuation system for the model is given in reference 10.

In order to perform analytical calculations for the model, it was necessary to specify a set of generalized masses, mode shapes, and natural frequencies. These properties were determined experimentally for the first nine structural modes of the model by using methods similar to those described in reference 11. The measured modal contours, natural frequencies, and generalized masses are given in figure 4.

Control Law

A simplified block diagram of the delta-wing flutter-suppression system is presented in figure 5. The control law used is of the form

$$\begin{Bmatrix} \beta \\ \delta \end{Bmatrix} = \begin{bmatrix} C_{11} & C_{12} \\ C_{21} & C_{22} \end{bmatrix} \begin{Bmatrix} h_1/b \\ \alpha \end{Bmatrix} + i \begin{bmatrix} G_{11} & G_{12} \\ G_{21} & G_{22} \end{bmatrix} \begin{Bmatrix} \dot{h}_1/b \\ \dot{\alpha} \end{Bmatrix} \quad (4)$$

where β is the leading-edge control deflection; δ is the trailing-edge control deflection; h_1 and α are the plunging and pitching motions, respectively, of a representative streamwise section of the wing (section A-A in fig. 5); b is a reference length; and C and G are constant coefficients which were evaluated from an aerodynamic-energy analysis.

The motions of h_1 and h_2 are measured by accelerometers located at 30 and 70 percent of the local chord c . The control law is mechanized on an analog computer which has been programmed to perform the operations indicated in figure 5 to determine h_1 , \dot{h}_1 , α , and $\dot{\alpha}$, and pass the proper command signal as expressed in equation (4) to the control surfaces. Figure 5 indicates that the period of oscillation $1/\omega$ must be determined. However, reference 3 showed that essentially the same results can be obtained if the value of $1/\omega$ is taken to be constant and equal to the open-loop flutter period. This result was confirmed by preliminary wind-tunnel investigations.

Flutter Analysis

In order to illustrate the mechanism of flutter suppression, a flutter analysis, both with and without active controls, is presented. The flutter equations for a three-dimensional lifting surface are obtained from Lagrange's equation of motion by assuming that the unknown mode of motion is described by a linear combination of orthogonal modes, that is, the undamped natural modes of the system, in the following manner:

$$h(x,y,t) = \sum_{i=1}^n q_i(t) Z_i(x,y) \quad (5)$$

If structural damping is neglected, then the equations of motion become

$$M_i \ddot{q}_i(t) + \omega_i^2 M_i q_i(t) = Q_i(t) \quad (6)$$

where

$$M_i = \iint_S m(x,y) Z_i^2(x,y) dx dy$$

is the generalized mass and

$$Q_i(t) = \iint_S \Delta p(x,y,t) Z_i(x,y) dx dy$$

is the generalized aerodynamic force. The total pressure distribution $\Delta p(x,y,t)$ is composed of contributions due to each flexible mode plus those due to the leading- and trailing-edge controls. Therefore,

$$\Delta p(x,y,t) = \sum_{j=1}^n \Delta p_j(x,y) q_j(t) + \Delta p_\delta^\delta + \Delta p_\beta^\beta$$

where Δp_j is the pressure distribution due to each flexible mode, and Δp_β and Δp_δ are the pressure distributions due to leading- and trailing-edge controls, respectively. Substituting this expression for the pressures into equation (6) and expanding results in the following form of the equations of motion:

$$\begin{aligned} (-\omega^2 M_i + \omega_i^2 M_i) q_i(t) &= \sum_{j=1}^n \left(q_j(t) \iint_S \Delta p_j Z_i dx dy \right) \\ &+ \beta \iint_S \Delta p_\beta Z_i dx dy + \delta \iint_S \Delta p_\delta Z_i dx dy \end{aligned} \quad (7)$$

From equation (5), the nondimensionalized deflection of the wing for the responses h_1 and h_2 can be written as

$$\frac{h_1}{b} = \frac{1}{b} \sum_{i=1}^n q_i(t) Z_i(x_1, y_1) \quad \frac{h_2}{b} = \frac{1}{b} \sum_{i=1}^n q_i(t) Z_i(x_2, y_2)$$

Assuming that a straight line between the locations of the two sensors gives a reasonable approximation to the angle of attack at the reference station and noting that the sensors are $0.8b$ apart lead to the following equation for angle of attack:

$$\alpha = \frac{1}{0.8} \left(\frac{h_2}{b} - \frac{h_1}{b} \right) = \frac{1}{0.8b} \sum_{i=1}^n (Z_i(x_2, y_2) - Z_i(x_1, y_1)) q_i(t)$$

Substituting the above results into the control law (eq. (4)) results in a matrix equation relating the control-surface motions to the generalized coordinates in the following form:

$$\begin{Bmatrix} \beta \\ \delta \end{Bmatrix} = \begin{bmatrix} A_1 + iB_1 & A_2 + iB_2 & \dots & A_n + iB_n \\ C_1 + iD_1 & C_2 + iD_2 & \dots & C_n + iD_n \end{bmatrix} \begin{Bmatrix} q_1 \\ q_2 \\ \vdots \\ q_n \end{Bmatrix} \quad (8)$$

where the parameters A_i , B_i , C_i , and D_i are constant coefficients defined as follows:

$$A_i = Z_i(x_1, y_1) \left(\frac{C_{11}}{b} - \frac{C_{12}}{0.8b} \right) + Z_i(x_2, y_2) \frac{C_{12}}{0.8b}$$

$$B_i = Z_i(x_1, y_1) \left(\frac{G_{11}}{b} - \frac{G_{12}}{0.8b} \right) + Z_i(x_2, y_2) \frac{G_{12}}{0.8b}$$

$$C_i = Z_i(x_1, y_1) \left(\frac{C_{21}}{b} - \frac{C_{22}}{0.8b} \right) + Z_i(x_2, y_2) \frac{C_{22}}{0.8b}$$

$$D_i = Z_i(x_1, y_1) \left(\frac{G_{21}}{b} - \frac{G_{22}}{0.8b} \right) + Z_i(x_2, y_2) \frac{G_{22}}{0.8b}$$

Substituting equation (8) into equation (7) results in the final form of the equations of motion:

$$\begin{aligned} (-\omega^2 M_i + \omega_i^2 M_i) q_i(t) = & \sum_{j=1}^n q_j \left(\iint_S \Delta p_j Z_i \, dx \, dy + (A_j + iB_j) \iint_S \Delta p_\beta Z_i \, dx \, dy \right. \\ & \left. + (C_j + iD_j) \iint_S \Delta p_\delta Z_i \, dx \, dy \right) \end{aligned} \quad (9)$$

It should be noted from the form of the equations presented here that the active controls serve only to modify the aerodynamic forces of the wing alone. The Hermitian matrix U described earlier can be derived directly from the aerodynamic terms appearing in this equation and the effect of active controls on this matrix determined. Flutter calculations without active controls are performed by setting the coefficients A , B , C , and D equal to zero.

Flutter calculations were performed for the delta-wing model at Mach numbers of 0.6, 0.7, 0.8, and 0.9. The generalized aerodynamic forces appearing in equation (9) were formulated through the use of doublet-lattice aerodynamics as described in reference 12. This method requires the subdivision of the lifting surface into an array of trapezoidal boxes arranged in streamwise columns with a line of pulsating doublets located at the quarter chord of each box. The geometric boundary condition of tangential flow is satisfied at the 3/4-chord location for each box. The delta-wing model was divided into 160 boxes arranged in 16 streamwise strips with 10 boxes per strip. This arrangement provided six boxes on each control surface. All flutter calculations were made using the first nine measured structural modes, generalized masses, and natural frequencies. It should be noted that the equations of motion did not include control-surface dynamics since the natural frequency of rotation for each surface was considerably above the frequency of interest.

Results

Flutter. - Flutter characteristics of the model without active controls were experimentally determined in the Langley transonic dynamics tunnel at Mach numbers of 0.6, 0.7, 0.8, and 0.9. For these tests the control surfaces were kept at 0° deflection by applying hydraulic pressure to the actuators. The pressurized system acted as a very stiff spring and kept the rotational frequencies of the controls many times higher than the flutter frequency. Once the flutter boundary of the wing was established, an evaluation of the effect of active controls on raising the boundary was begun. However, these studies were conducted only at a Mach number of 0.9 because of an unexplained high-frequency, large-amplitude oscillation of the leading-edge control above a certain range of dynamic pressure at the lower Mach numbers. This phenomenon occurred around 65 Hz, whereas the flutter frequency was 11 to 12.5 Hz. This problem is not believed to be a result of the control law, since this motion is also observed with the control loop open, but has been introduced in some manner by the mechanization of the controls on the model.

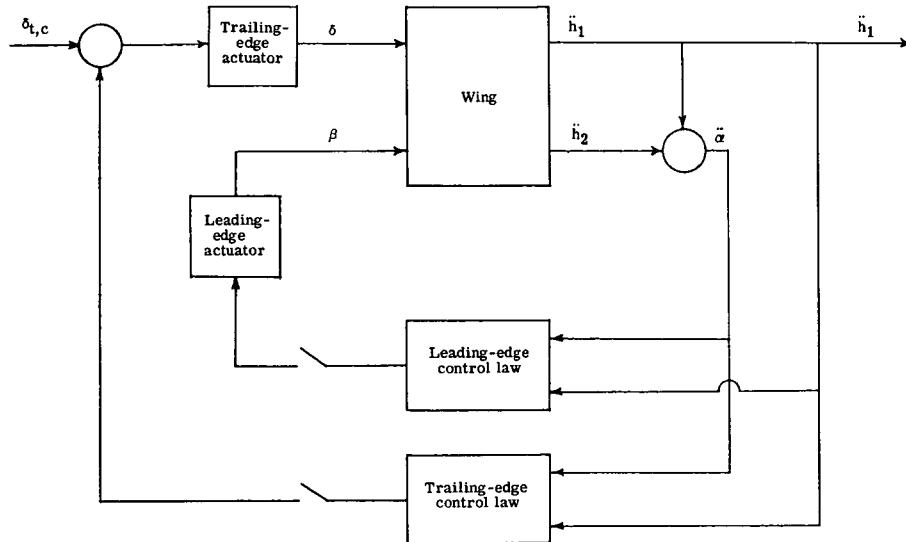
The experimental flutter results are presented in figure 6. At a Mach number of 0.9 the basic wing model fluttered at a dynamic pressure of 5.879 kN/m^2 . With active controls the flutter point was raised to 6.607 kN/m^2 , reflecting an increase of approximately 12 percent in dynamic pressure. The degree of confidence in the control system was such that when open-loop flutter was encountered, the active control loop was closed

to suppress the motion. The observed flutter motions for both open- and closed-loop operation were similar in nature and closely resembled the second natural vibration mode with some slight primary bending.

A comparison of calculated and experimental data is also presented in figure 6. The calculations for the basic wing show excellent agreement at all Mach numbers; however, the calculations with active controls predict a higher flutter point than was measured. At a Mach number of 0.9 the calculated increase in flutter dynamic pressure was approximately 21 percent compared with the measured increase of 12 percent. This difference is believed to be due to the inability of the aerodynamic theory to predict adequately the pressure distributions resulting from actuating the control surfaces, the lack of control-surface dynamics in the equations of motion, and the amplitude and phase lags incurred between the desired and actual control-surface deflections introduced by implementing the control loop on the model.

On the basis of these calculated results, it was decided to investigate analytically the sensitivity of the system to phase lag between the desired and actual control-surface deflections. A separate set of calculations were made which included a phase lag for both leading- and trailing-edge controls. The phase angle was experimentally determined for the model by measuring the frequency response of the actuator systems. At the flutter frequency of about 12 Hz, both surfaces had a phase lag of approximately 18° , and this value was used in the calculations. The results of these calculations are presented in figure 6. At a Mach number of 0.9 the phase angle reduced the increase in flutter dynamic pressure from 21 percent to 16 percent and resulted in a more favorable comparison with experiment.

Subcritical response.- In order to explore fully the behavior of the model below the flutter boundaries, two techniques for estimating the damping associated with the flutter mode were used. The first of these techniques (described in ref. 13) involves measuring the forced response of the model to an input generated by the trailing-edge controls as indicated in sketch 1. A measure of the damping in each mode can be obtained for both open- and closed-loop operation if the transfer function relating the forced response to the command signal $(\ddot{h}_1/\delta_{t,c})$ is determined as a function of frequency. During the wind-tunnel test an electronic signal analyzer was used to determine the in-phase and out-of-phase components of the response h_1 with respect to the trailing-edge command signal. Figure 7 presents a typical plot of this response at a Mach number of 0.9 and a dynamic pressure of 5.429 kN/m^2 . The curves in the upper portion of this figure represent the response of the basic wing; the lower curves, the response with the control loop closed. The damping in the modes can be estimated from the out-of-phase component by the frequencies labeled f_A and f_B . For an equivalent system with a single degree of freedom, these



Sketch 1

are the frequencies at the half-power points, and the damping can be expressed in terms of these frequencies:

$$g = \frac{\left(\frac{f_A}{f_B}\right)^2 - 1}{\left(\frac{f_A}{f_B}\right)^2 + 1}$$

The data shown in figure 7 are for a 3-minute logarithmic sweep from 5 to 25 Hz.

A qualitative measure of the effect of active controls in reducing the forced response of the system is evident from figure 7. The closed-loop system significantly alters the response by adding appreciable damping to the model. However, a quantitative measure of the damping is quite difficult to estimate because of the noise in the signal resulting from the model responding to tunnel turbulence. As the dynamic pressure is further increased, the signal-to-noise ratio becomes extremely high and results in very poor response plots. For this model the forced-response technique did not provide very useful information, but it will be shown later that this procedure can be an extremely useful tool in estimating the subcritical response.

The second technique that was used is referred to as "randomdec" and is described in reference 14. Basically, the technique extracts the damped sinusoidal response of the model vibration modes from the response of the model to tunnel turbulence. This is accomplished by assuming that the measured response is composed of the response to a step, an impulse, and a random force. By averaging the measured response over a number of time sweeps, the response of the system to a step is determined, since the response

to an impulse and to a random force average to zero. Damping is then obtained in the same manner as from a free-vibration decay which would be obtained if the model were given an initial displacement in the critical mode and then released. For a system with multiple degrees of freedom a filter is required to isolate the modes of interest. It should be pointed out that when the frequencies of the structural modes are closely spaced, both the randomdec and forced-response techniques suffer from the problem of accurately determining the damping value.

The randomdec technique was used to obtain the plot in figure 8, which is the measured system damping in the critical flutter-mode frequency range as a function of dynamic pressure at a Mach number of 0.9. The hatched area represents the experimental scatter of the data. Typical randomdec signatures are presented at a dynamic pressure of 5.841 kN/m^2 , which is within 1 percent of the flutter dynamic pressure. The open-loop damping is about 0.008; the closed loop, about 0.075. Also shown are the measured open- and closed-loop flutter points. Because of the frequency spectrum of the structural modes of interest, this technique proved to be quite valuable in establishing the subcritical behavior of the model. For test conditions at which the forced-response technique described earlier gave meaningful results, these results also fell within the scatter indicated in figure 8.

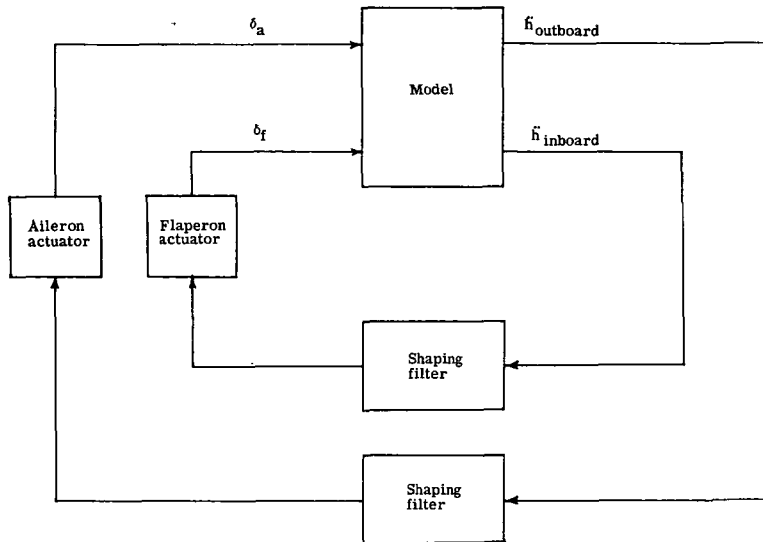
B-52 FLUTTER-SUPPRESSION PROGRAM

In addition to the delta-wing program, the Langley Research Center is engaged in a cooperative program with the Air Force Flight Dynamics Laboratory to study symmetric flutter suppression on a model of the B-52 CCV airplane. As mentioned in the Introduction, the B-52 program will include studies of the application of other active control systems including maneuver-load control, ride-quality control, and relaxed static stability.

Model Program

The model program uses a 1/30-size dynamically and aeroelastically scaled model of the B-52. A photograph of the model installed in the Langley transonic dynamics tunnel is shown in figure 9. In order to provide a simulation of the free-flight dynamics, the model is mounted on a modified version of the two-cable mount system described in reference 15. This mount provides the model with a soft support in that the natural frequencies associated with the mount are well below those of the free-flight and elastic modes.

The active flutter-suppression system designed for the model is indicated in the simplified block diagram shown in sketch 2. This control system was not designed with the use of the energy approach discussed earlier. It is a result of previous experience and analysis of the B-52 which have indicated that aerodynamic forces on the wing are



Sketch 2

stabilizing for 360° of the flutter oscillation cycle when the incremental lift generated by the control surfaces lags the wing motion by 90° . The control law is essentially a shaping filter which provides the required phase lag between wing lift and displacement at the flutter frequency. A summary of the analysis, synthesis, and hardware implementation being used for the flight program is presented in reference 16.

As indicated in sketch 2, the control system incorporates an active flaperon and outboard aileron. The placement of these controls is indicated in figure 10. An outboard accelerometer is used to drive the ailerons. A second inboard accelerometer is used to drive the flaperons. Because of the smaller hinge moments required for this model and the substantially larger volume available than in the delta-wing model, an electromechanical system was designed to actuate the controls. This system consisted of separate dc torque motors mounted within the fuselage to drive the ailerons and flaperons. The linkages used to drive the controls were designed to isolate them from the structure so that they would not change the stiffness characteristics of the wing. A description of this system is presented in reference 10.

Results

Experimental studies of the B-52 model were performed in the Langley transonic dynamics tunnel. The prime objectives of these tests were to establish the behavior of the flutter-suppression system below the flutter boundary. A plot of estimated damping in the critical flutter mode (approximately 12.8 Hz), using the forced-response technique, against tunnel dynamic pressure is presented in figure 11. Experimental results for the open-loop system, the closed-loop system with nominal gains, and the closed-loop system

with double the nominal gains are indicated in this figure. It is readily apparent from these results that the effect of active controls is appreciable. Even with nominal gains, the damping at a dynamic pressure 2.42 kN/m^2 is more than double that of the open-loop system. With twice the nominal gains, not only has the level of damping increased but even the trend with increasing dynamic pressure has reversed direction.

A typical plot of the measured in-phase and out-of-phase response of the model is presented in figure 12. For this model the ailerons were used to generate the forcing function. As indicated in figure 12 the damping was estimated by determining the ratio of the outboard-accelerometer response to the aileron command for a frequency range of 4 to 24 Hz. The randomdec technique did not provide useful results until the model was tested near the flutter boundary, at which time most of the wing response was predominantly in the lowly damped flutter mode.

CONCLUDING REMARKS

A description of two wind-tunnel studies used to evaluate active control of flutter suppression has been presented. A flutter-suppression method based on an aerodynamic-energy criterion has been described, and some results of the application of this method to a simplified delta-wing model are presented. An increase of approximately 12 percent in the flutter dynamic pressure for this model has been achieved at a Mach number of 0.9 through the use of leading- and trailing-edge controls. Analytical calculations have been compared with experiment and indicate excellent agreement for the open-loop system; however, calculations for the closed-loop system predicted a larger increase in dynamic pressure than was measured.

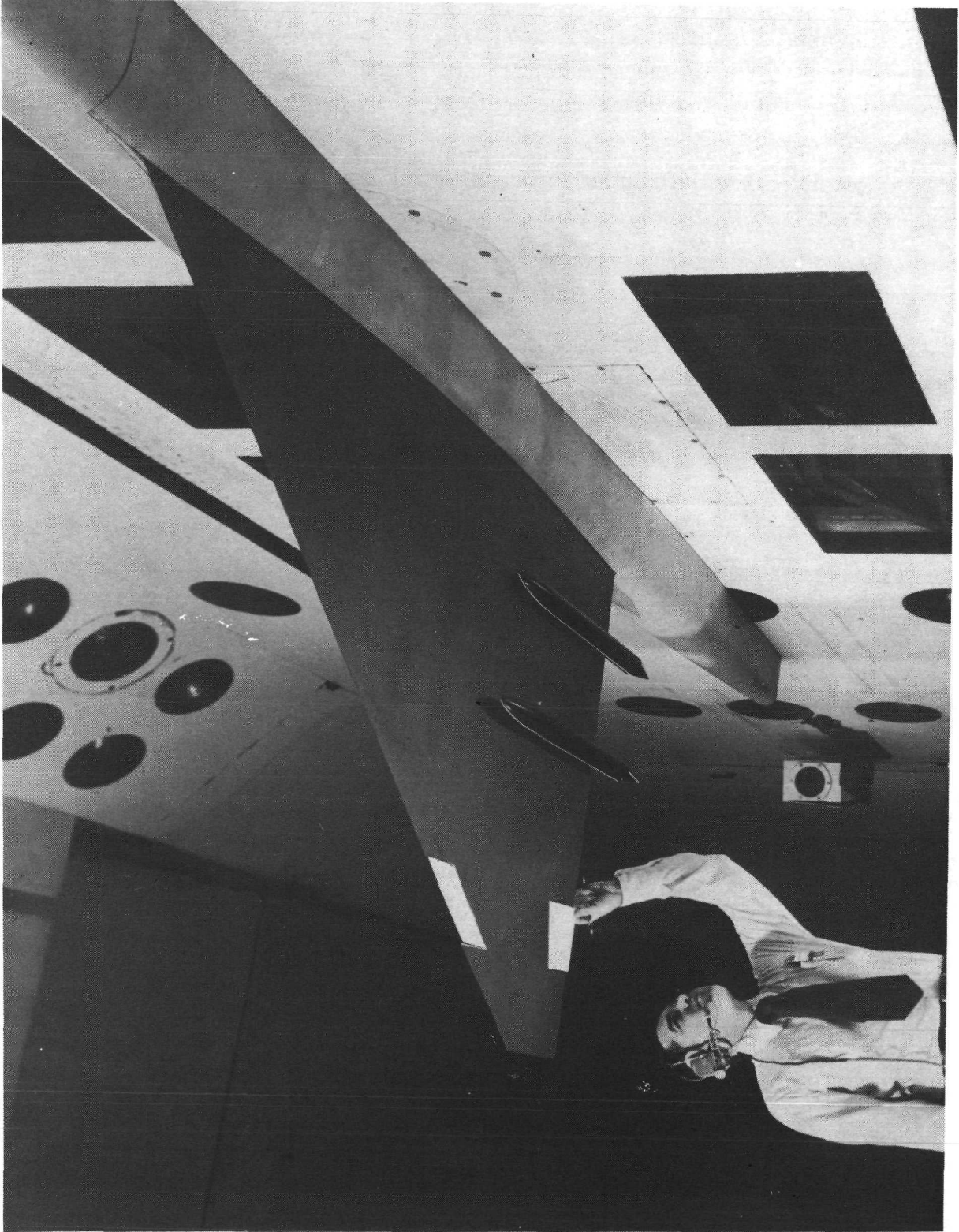
Some preliminary experimental results of a flutter-suppression study of an aeroelastic model of the B-52 CCV airplane have been presented. A flutter-suppression method based on the phasing between wing motion and control-surface deflections has indicated that significant improvements in the subcritical damping of the flutter mode can be achieved through the use of active controls.

Langley Research Center,
National Aeronautics and Space Administration,
Hampton, Va., August 27, 1973.

REFERENCES

1. Wykes, John H.; and Kordes, Eldon E.: Analytical Design and Flight Tests of a Modal Suppression System on the XB-70 Airplane. *Aeroelastic Effects From a Flight Mechanics Standpoint*, AGARD CP-46, 1970, pp. 23-1 - 23-18.
2. Burris, P. M.; Dempster, J. B.; and Johannes, R. P.: Flight Testing Structural Performance of the LAMS Flight Control System. *AIAA Paper No. 68-244*, Mar. 1968.
3. Nissim, E.: Flutter Suppression Using Active Controls Based on the Concept of Aerodynamic Energy. *NASA TN D-6199*, 1971.
4. Triplett, William E.; Kappus, Hans-Peter F.; and Landy, Robert J.: Active Flutter Control: An Adaptable Application to Wing/Store Flutter. *AIAA Paper No. 73-194*, Jan. 1973.
5. Thompson, Glenn O.; and Kass, Gerald J.: Active Flutter Suppression - An Emerging Technology. *J. Aircraft*, vol. 9, no. 3, Mar. 1972, pp. 230-235.
6. Rainey, A. Gerald; Ruhlin, Charles L.; and Sandford, Maynard C.: Active Control of Aeroelastic Response. *Stability and Control*, AGARD CP-119, 1972, pp. 16-1 - 16-5.
7. Kass, Gerald J.; and Johannes, R. P.: B-52 Control Configured Vehicles Program. *AIAA Paper No. 72-747*, Aug. 1972.
8. Hunt, Gerald L.; and Walberg, Gerald D.: Calculated Mode Shapes and Pressure Distributions at Flutter for a Highly Tapered Horizontal Tail in Subsonic Flow. *NASA TN D-1008*, 1962.
9. Garrick, I. E.: Perspectives in Aeroelasticity. *Israel J. Technol.*, vol. 10, no. 1-2, 1972, pp. 1-22.
10. Bergmann, Gerald E.; and Severt, Francis D.: Design and Evaluation of Miniature Control Surface Actuation Systems for Aeroelastic Models. *AIAA Paper No. 73-323*, Mar. 1973.
11. Abel, Irving: A Wind-Tunnel Evaluation of Analytical Techniques for Predicting Static Stability and Control Characteristics of Flexible Aircraft. *NASA TN D-6656*, 1972.
12. Albano, Edward; and Rodden, William P.: A Doublet-Lattice Method for Calculating Lift Distributions on Oscillating Surfaces in Subsonic Flows. *AIAA J.*, vol. 7, no. 2, Feb. 1969, pp. 279-285.
13. Keller, Anton C.: Vector Component Techniques: A Modern Way To Measure Modes. *Sound & Vib.*, vol. 3, no. 3, Mar. 1969, pp. 18-26.

14. Cole, Henry A., Jr.: On-Line Failure Detection and Damping Measurement of Aerospace Structures by Random Decrement Signatures. NASA CR-2205, 1973.
15. Reed, Wilmer H., III; and Abbott, Frank T., Jr.: A New "Free-Flight" Mount System for High-Speed Wind-Tunnel Flutter Models. Proceedings of Symposium on Aeroelastic & Dynamic Modeling Technology, RTD-TDR-63-4197, Pt. 1, U.S. Air Force, Mar. 1964, pp. 169-206.
16. Hodges, Garold E.: Active Flutter Suppression - B-52 Controls Configured Vehicle. AIAA Paper No. 73-322, Mar. 1973.



L-73-355

Figure 1.- Delta-wing flutter-suppression model.

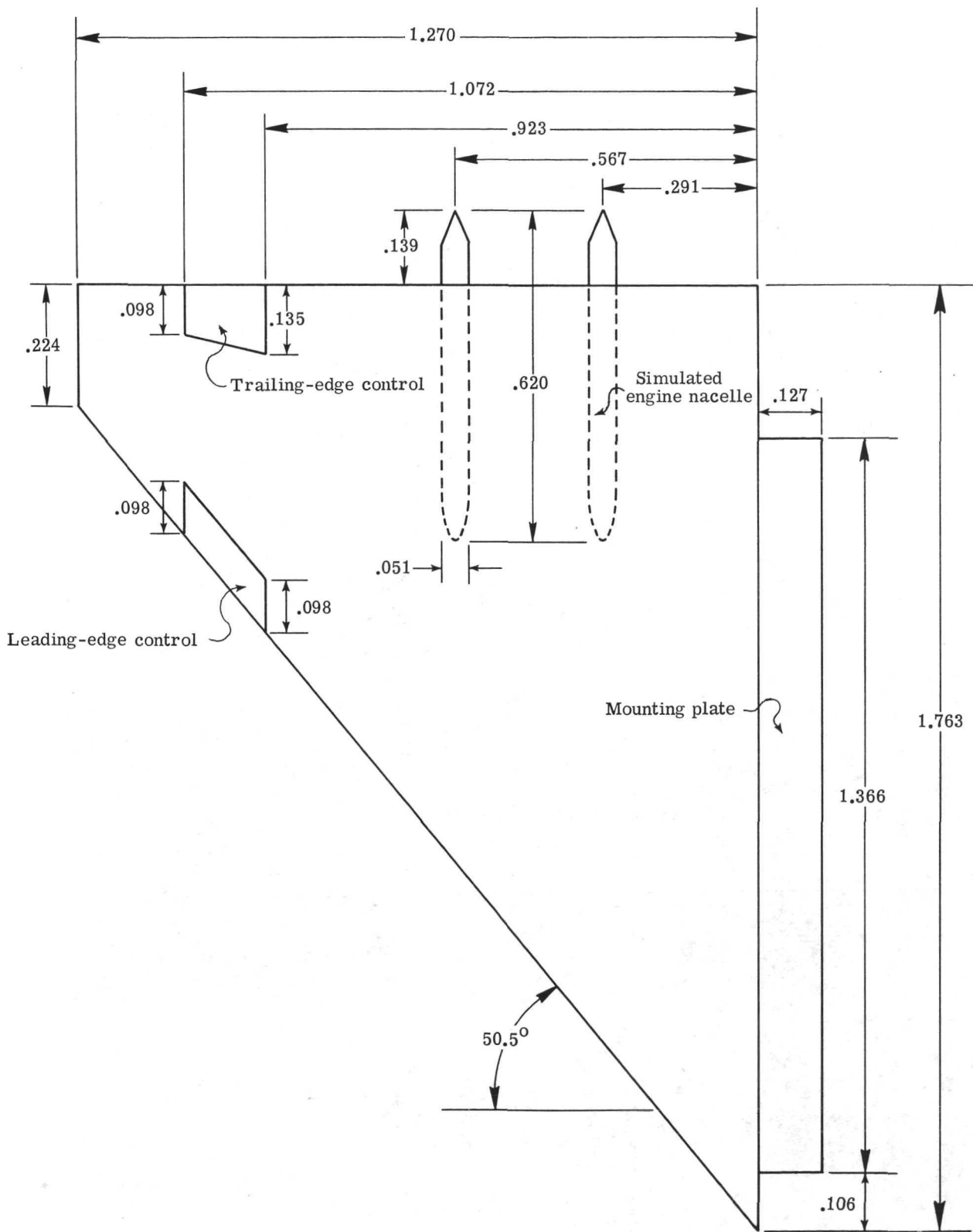
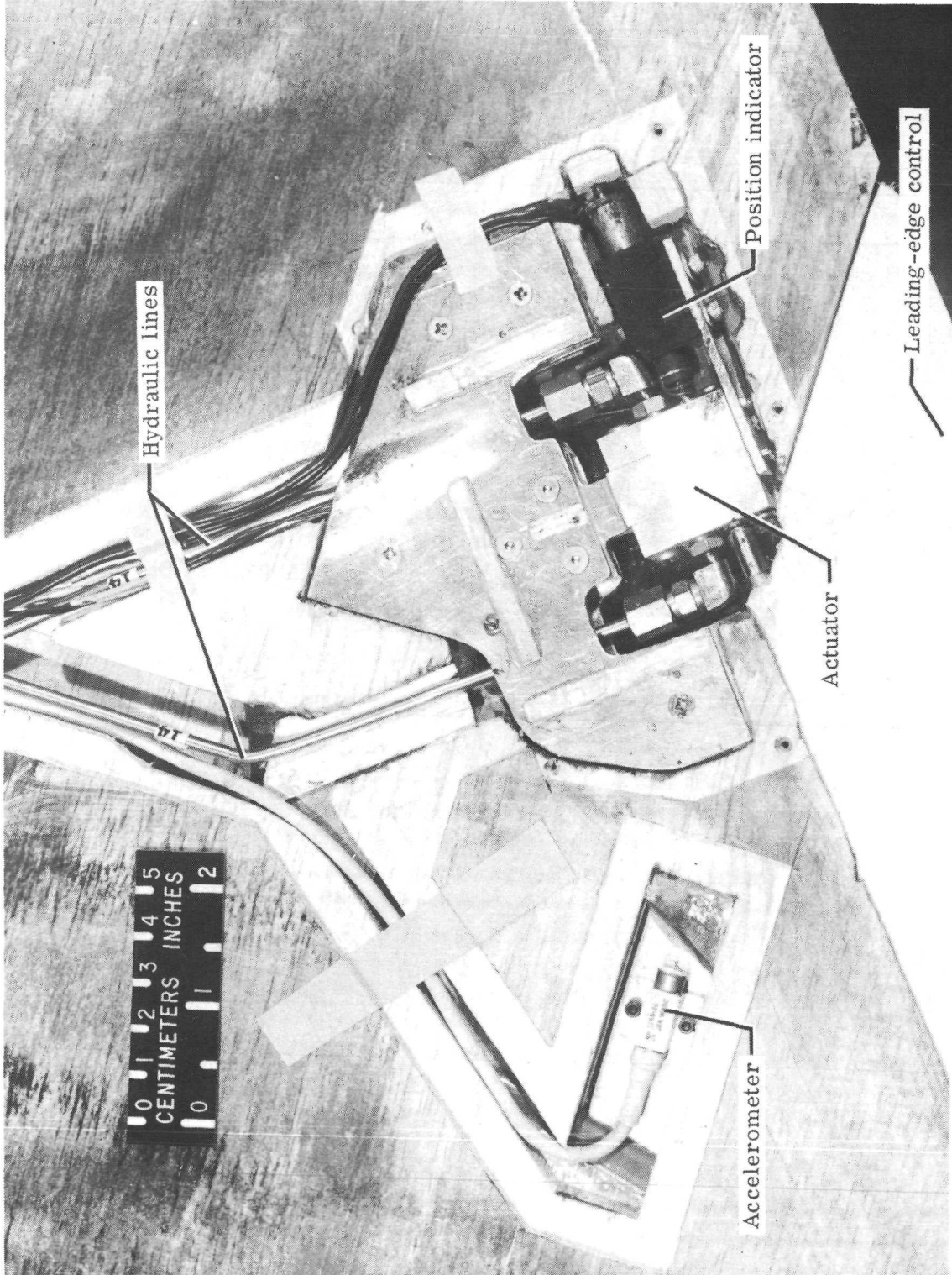


Figure 2.- Sketch of delta-wing model. (All linear dimensions are in meters.)



L-72-7362

Figure 3.- Delta-wing control system.

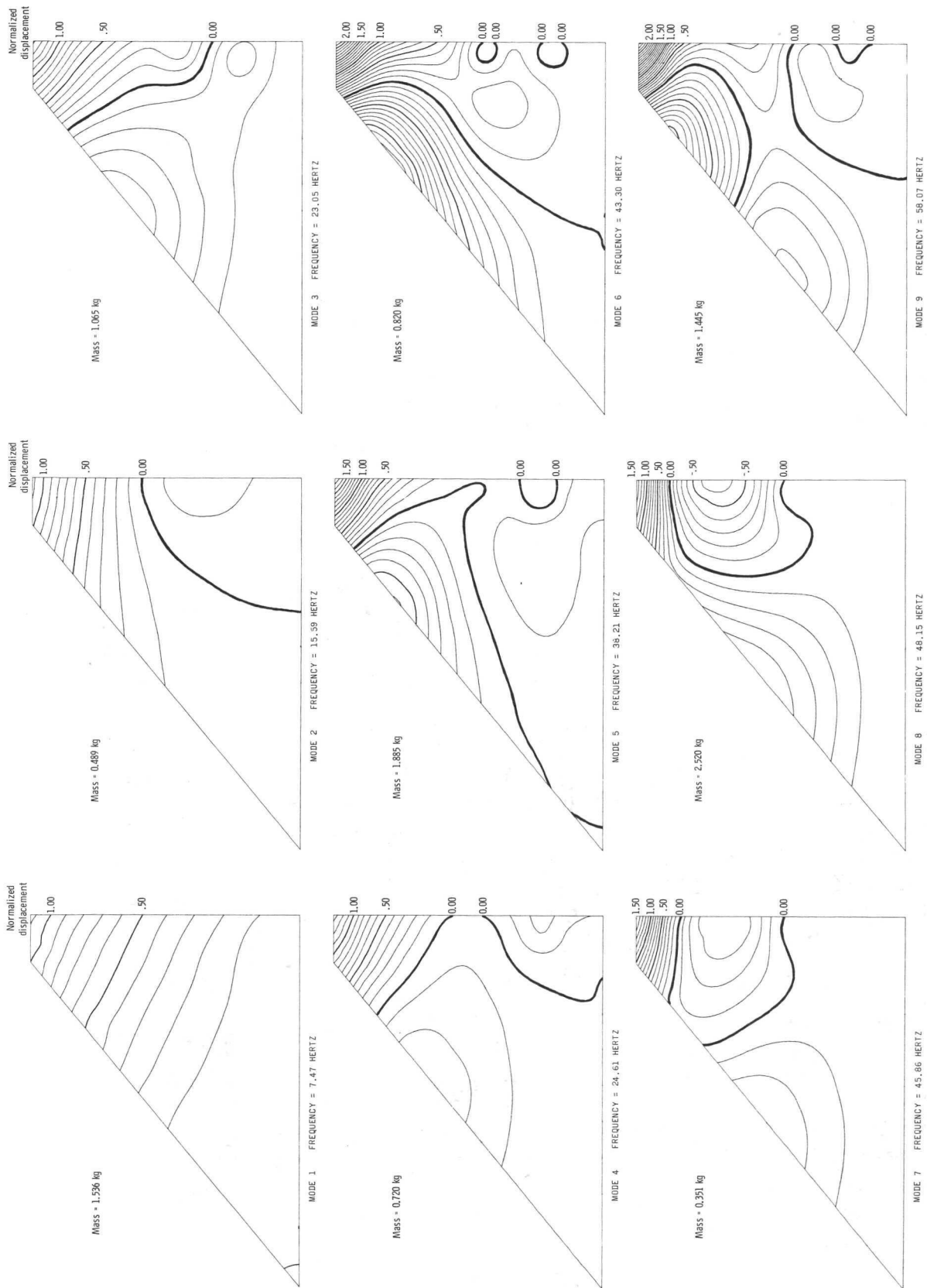


Figure 4.- Measured modal contours, generalized masses, and frequencies of natural vibration modes. (Contour interval, 0.1 normalized displacement.)

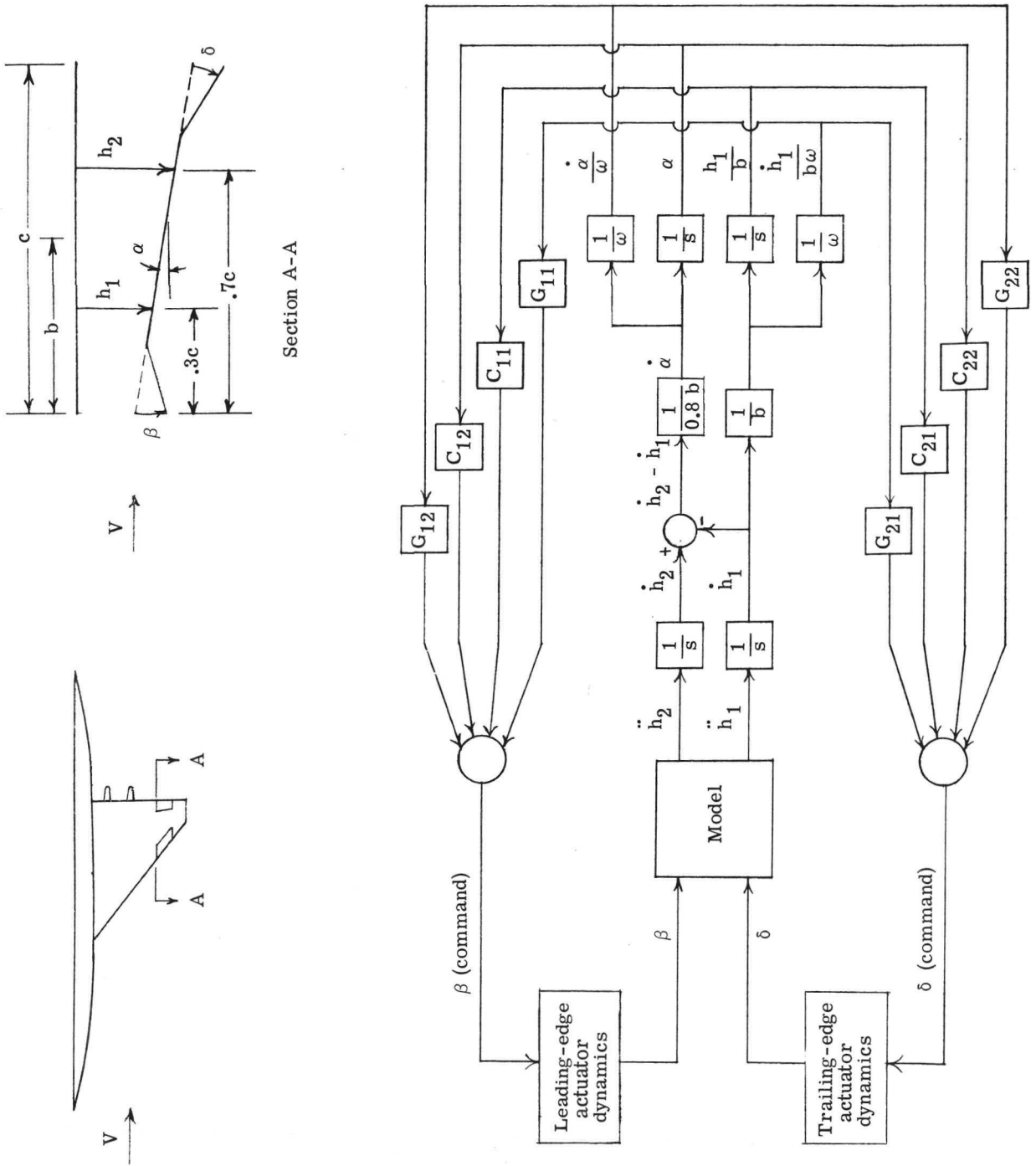


Figure 5.- Block diagram of flutter-suppression system.

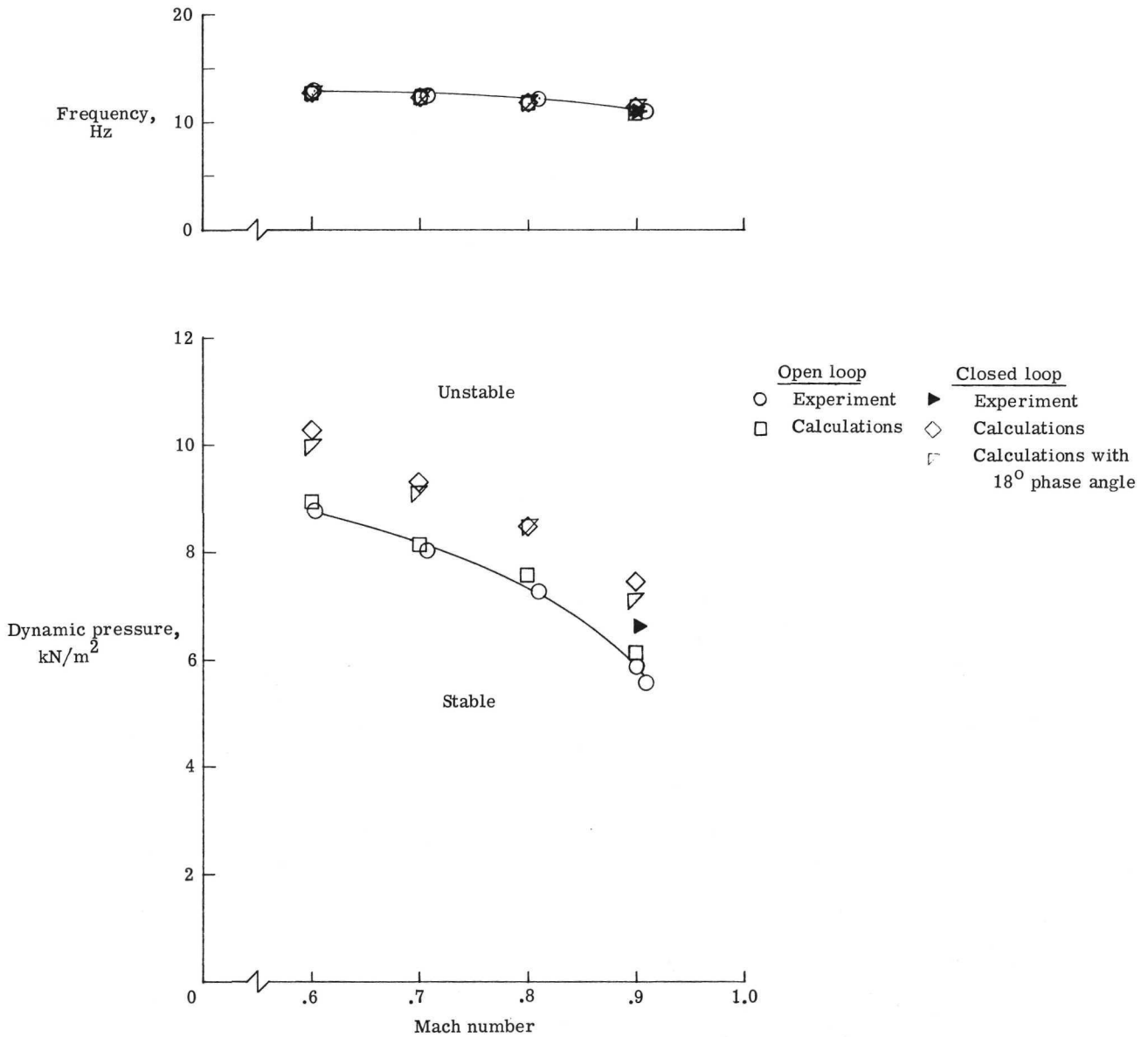
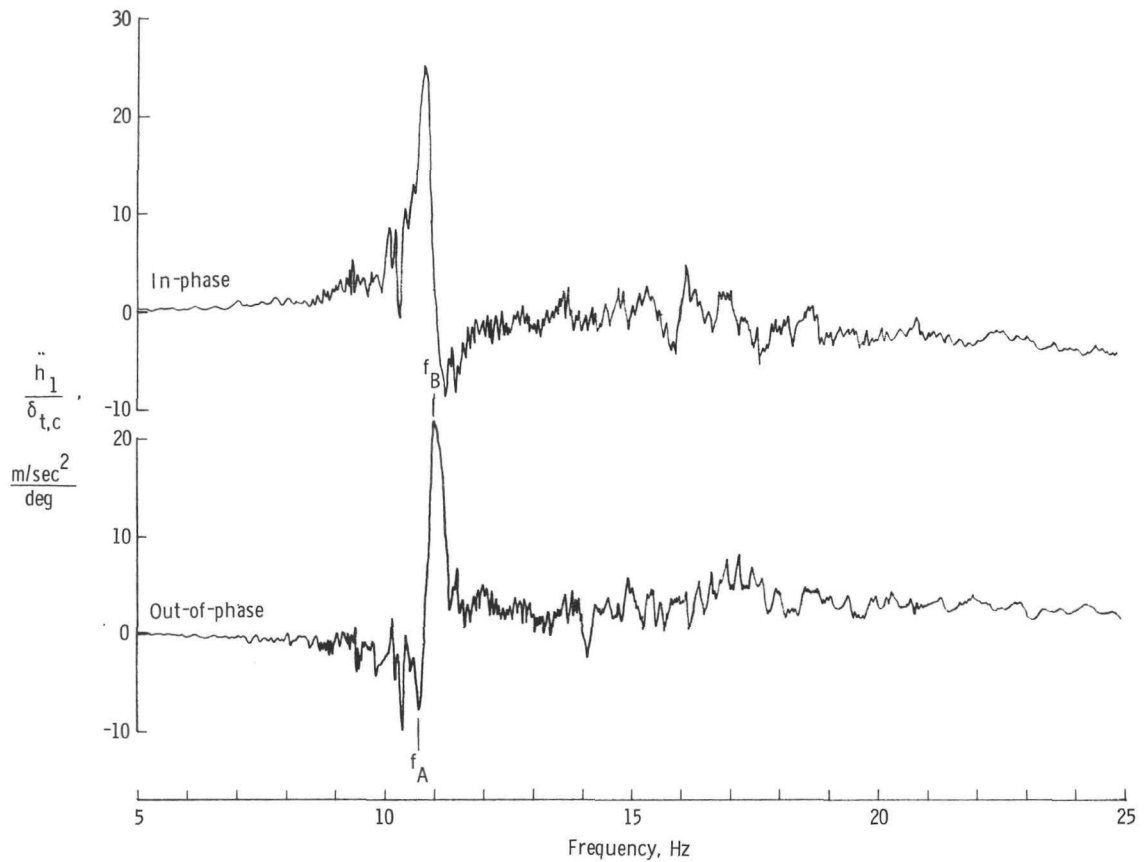
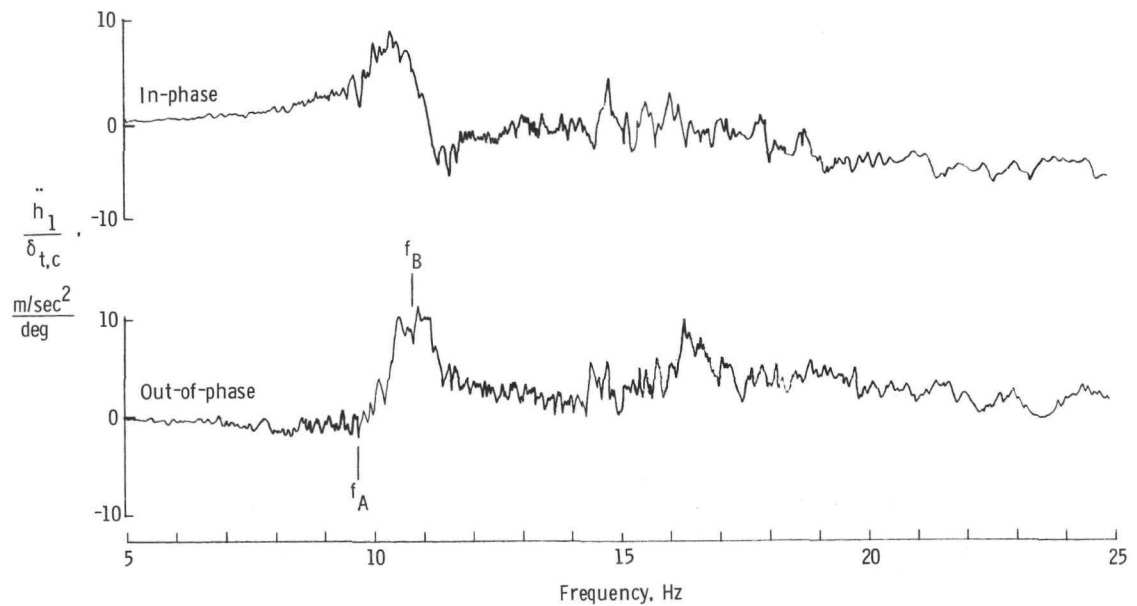


Figure 6.- Measured and calculated model flutter boundaries.



(a) Open-loop response. $g = 0.037$.



(b) Closed-loop response. $g = 0.107$.

Figure 7.- Measured forced response of model to trailing-edge-control excitation at Mach number of 0.9 and dynamic pressure of 5.429 kN/m².



Figure 8.- Measured subcritical damping at Mach number of 0.9.

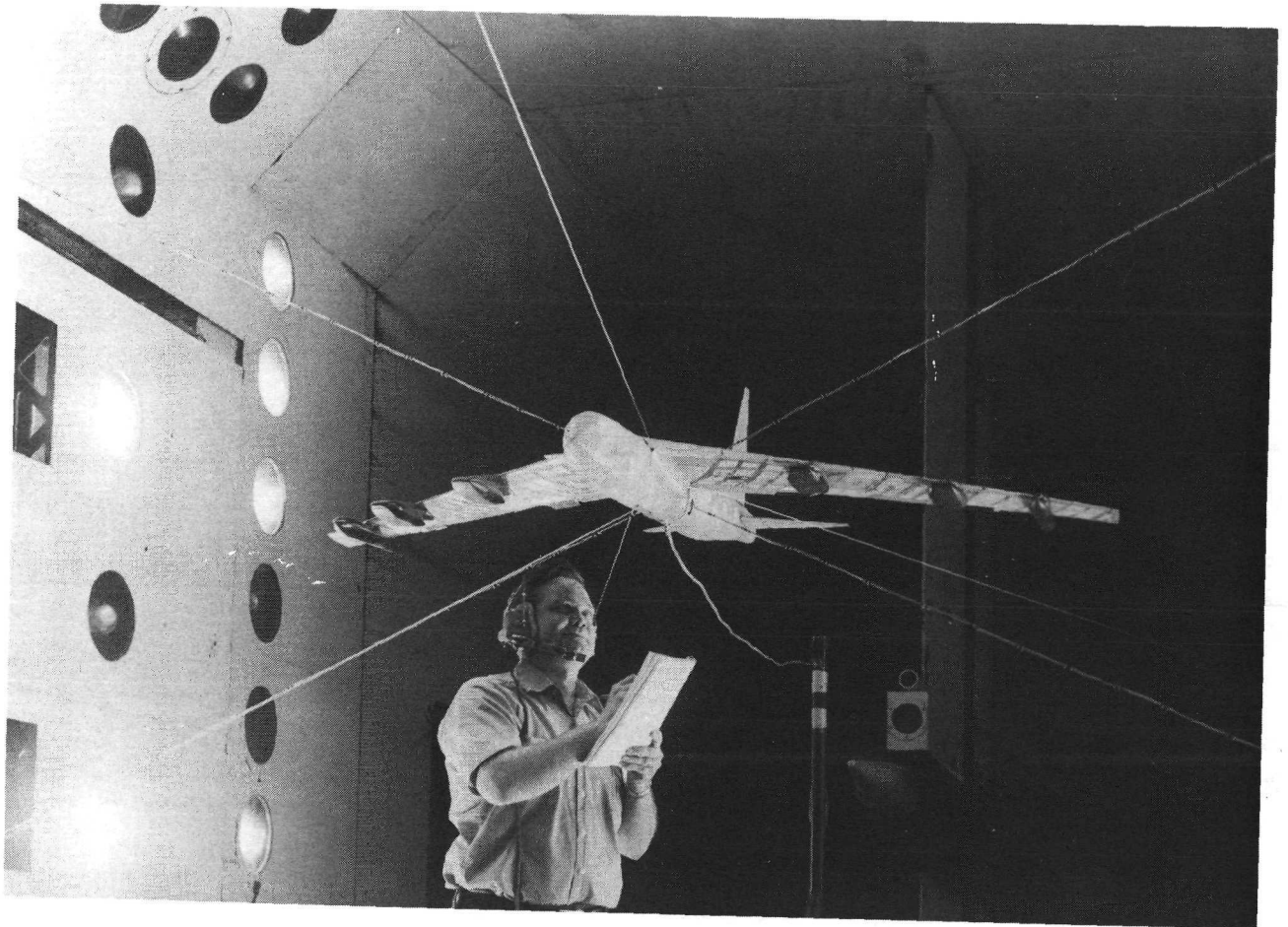


Figure 9.- B-52 CCV model mounted in the Langley transonic dynamics tunnel. L-73-4454

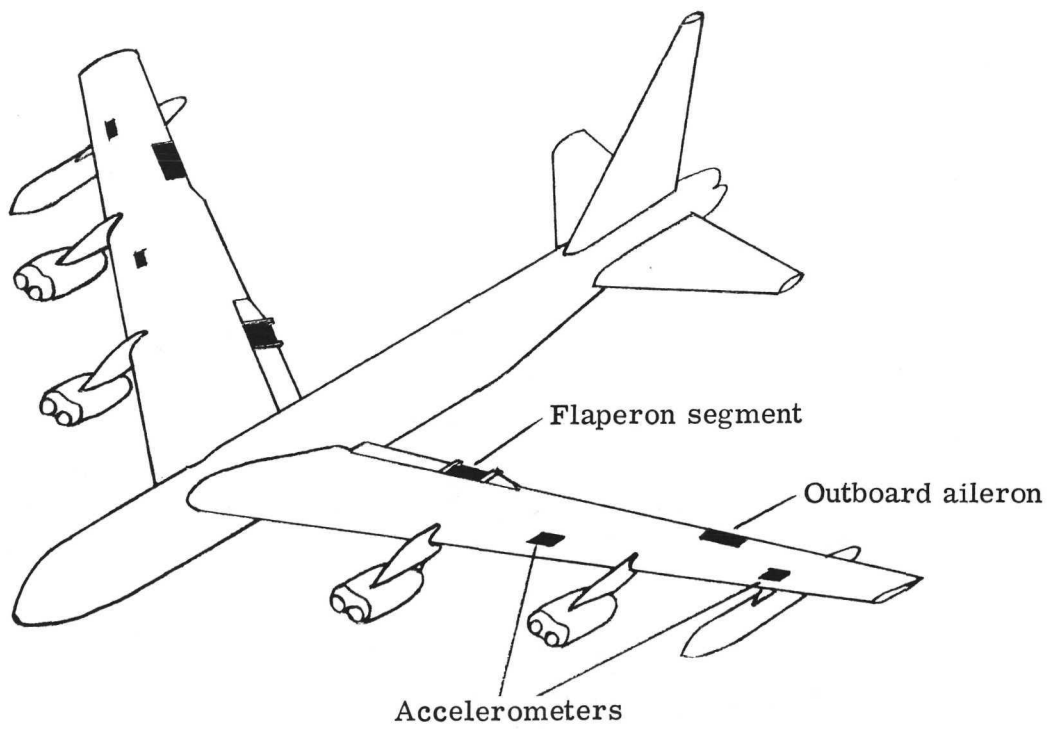


Figure 10.- B-52 model control surfaces used for flutter suppression.

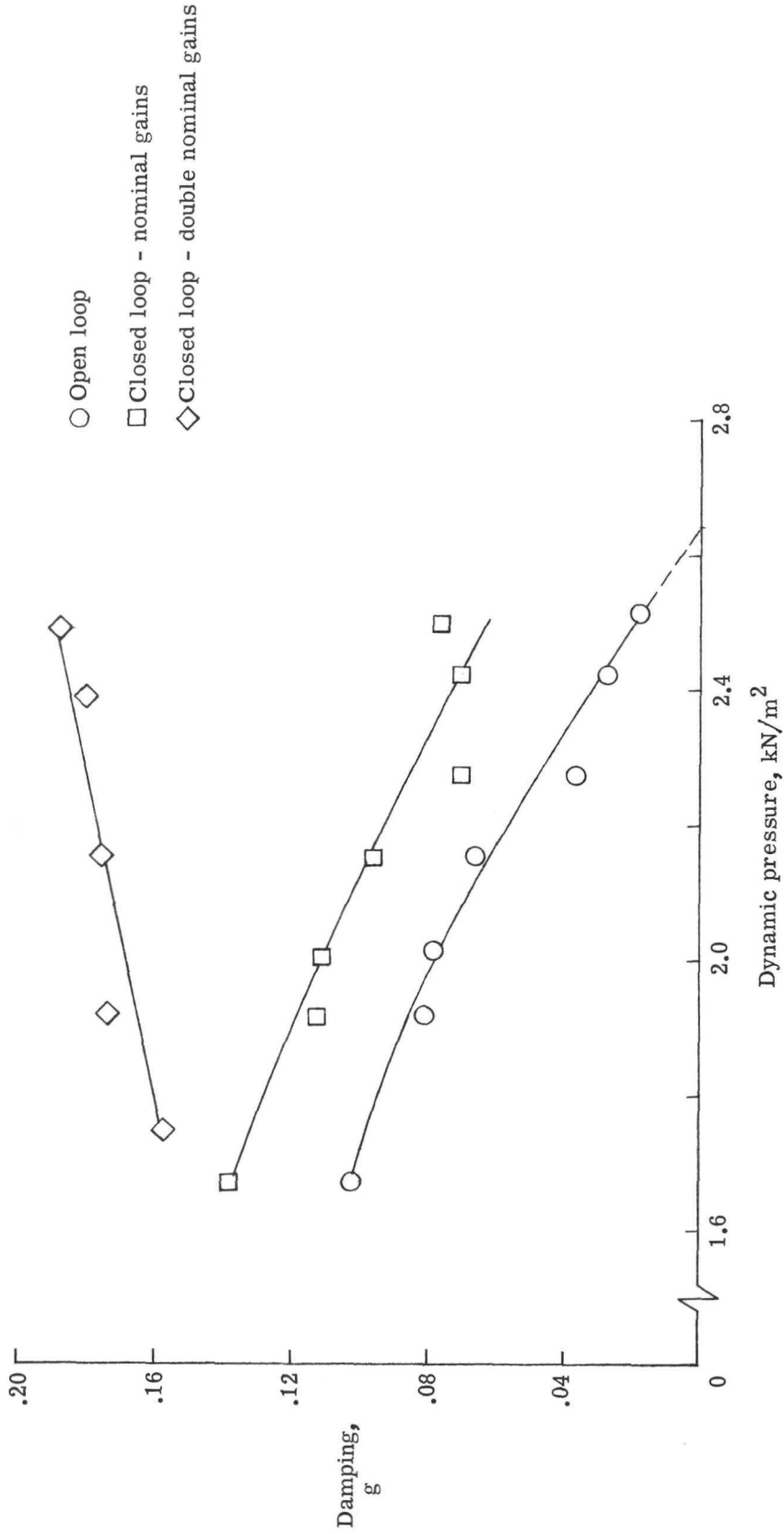
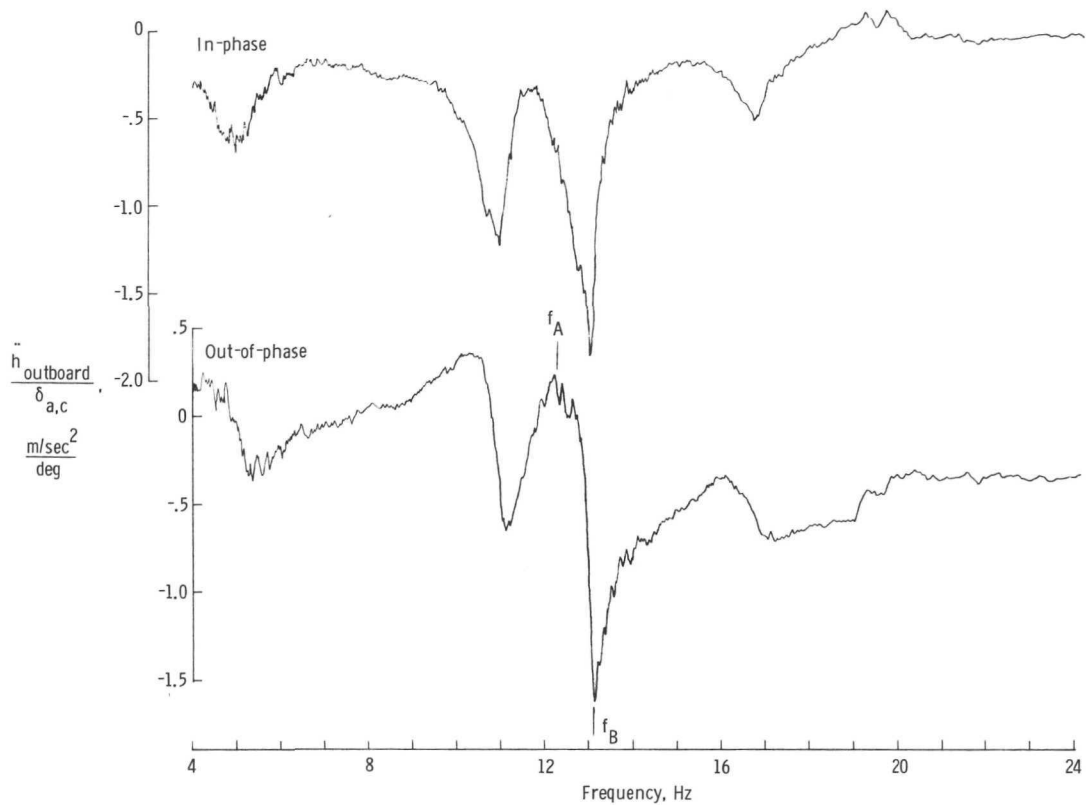
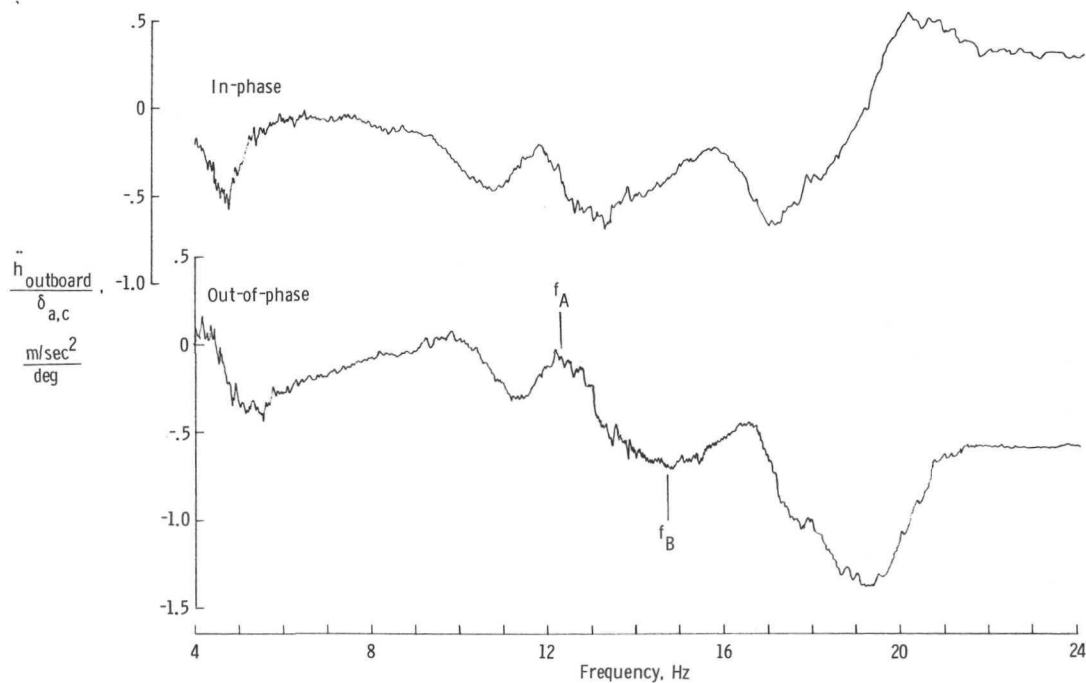


Figure 11.- Measured damping for B-52 flutter-suppression model.



(a) Open-loop response. $g = 0.062$.



(b) Closed-loop response – double nominal gains. $g = 0.176$.

Figure 12.- Measured forced response of B-52 model to aileron command at a dynamic pressure of 2.154 kN/m^2 .

NATIONAL AERONAUTICS AND SPACE ADMINISTRATION
WASHINGTON, D.C. 20546

OFFICIAL BUSINESS
PENALTY FOR PRIVATE USE \$300

SPECIAL FOURTH-CLASS RATE
BOOK

POSTAGE AND FEES PAID
NATIONAL AERONAUTICS AND
SPACE ADMINISTRATION
451



POSTMASTER: If Undeliverable (Section 158
Postal Manual) Do Not Return

"The aeronautical and space activities of the United States shall be conducted so as to contribute . . . to the expansion of human knowledge of phenomena in the atmosphere and space. The Administration shall provide for the widest practicable and appropriate dissemination of information concerning its activities and the results thereof."

—NATIONAL AERONAUTICS AND SPACE ACT OF 1958

NASA SCIENTIFIC AND TECHNICAL PUBLICATIONS

TECHNICAL REPORTS: Scientific and technical information considered important, complete, and a lasting contribution to existing knowledge.

TECHNICAL NOTES: Information less broad in scope but nevertheless of importance as a contribution to existing knowledge.

TECHNICAL MEMORANDUMS: Information receiving limited distribution because of preliminary data, security classification, or other reasons. Also includes conference proceedings with either limited or unlimited distribution.

CONTRACTOR REPORTS: Scientific and technical information generated under a NASA contract or grant and considered an important contribution to existing knowledge.

TECHNICAL TRANSLATIONS: Information published in a foreign language considered to merit NASA distribution in English.

SPECIAL PUBLICATIONS: Information derived from or of value to NASA activities. Publications include final reports of major projects, monographs, data compilations, handbooks, sourcebooks, and special bibliographies.

TECHNOLOGY UTILIZATION PUBLICATIONS: Information on technology used by NASA that may be of particular interest in commercial and other non-aerospace applications. Publications include Tech Briefs, Technology Utilization Reports and Technology Surveys.

Details on the availability of these publications may be obtained from:

**SCIENTIFIC AND TECHNICAL INFORMATION OFFICE
NATIONAL AERONAUTICS AND SPACE ADMINISTRATION
Washington, D.C. 20546**